ISSN No:-2456-2165 https://doi.org/10.38124/ijisrt/IJISRT24SEP075

Rice Husk Reuse in the Preparation of Biogenic SiO_2/TiO_2 and Nickel Hybrid Nanocomposites

Dr. A. Ananthi[1*]; K. Kapildev[2]
[1,2]Department of physics, Annamalai University, M.R.K. Arts and Science college, Kattumannar kovil (TK) , 608301

Corresponding Author:- Dr. A. Ananthi[1*]

Abstract:- In this study, biogenic SiO_2 of high purity and high surface area obtained from rice husk was used for prepare a nano structured RHS/TiO_2/Ni nanocomposite. The predominantly amorphous silica was extracted in an acidic method and then the nanocomposite was done via sol gel route adding Sodium hydroxide and nitric acid followed by combustion method. The chemical and physical properties of samples were analyzed by XRD, FTIR, UV, TEM, SEM/EDX and TG – DTA. The X-ray diffraction (XRD) of the nano composites had no characteristic property of SiO_2 and even anatase TiO_2 but indicated new crystal structures which were determined from the Fourier transform infrared spectrophotometer (FTIR) as a hybridized Ti – O – Si bonding. Thermo gravimetric analysis shows that the activation process can be divided into three parts based on the temperature zones. Furthermore the stabilization and formation of SiO_2/TiO_2 /Ni metal nano composites were confirmed by SEM/EDX and UV analysis. Thus, this paper may provide costless and easy procedure to synthesize new hybrid nanocomposite.

Keywords:- *Biogenic Silica, SiO_2/TiO_2/Ni Nanocomposite, Rice Husk.*

I. INTRODUCTION

Agro industry has generated a huge amount of residues and a necessity of utilization of these residues might reduce pollution and increase energy savings. [1,2]. SiO_2 can be obtained by direct calcination followed by calcination chemical treatment, and by sol-gel method. Titanium dioxide (TiO_2) is the naturally occurring oxide of titanium. It is a versatile transition – metal oxide and a useful material in various present/future applications. On the other way, silica plays the major role as a carrier of titania and enhances the surface area with enough pore size [4]. The modification of titania enhancing its catalytic performances can also be conducted by adding nitrogen, Cr and iodine. Silica from agro waste can be used as a natural silica source for the synthesis of titania – silica composites [5, 6]. This material was chosen because it is much cheaper than other oxides since this material is naturally available in large quantity.

In the previous research, adding titania to silica was conducted by using sodium silicate solution to titanium oxysulfate hydrate and results showed linkages between Si-O-Ti [11]. In the present investigation, the mixing titania to rice husk silica and template with the different concentrations of nickel was conducted by as a sol gel method where titanium tetra isopropoxide was used as titania source. In the present work is a combination of bio resource engineering and applied chemistry and would develop a latest method to protect the natural environment by utilizing useful bio resource in the vast environment.

II. EXPERIMENTAL DETAIL

➢ *Materials*

All the chemicals used were analytical reagnent. Titanium isopropoxide ($Ti(OC_3H_7)_4$ 97%) was used as a precursor of titania and Nickel nitride ($Ni(NO_3)_2.6H_2O$ as dopant sources. Other materials used were nitric acid and sodium hydroxide pellets. Rice husk gathered from agriculture department, Annamalai Univerrsity. All the chemicals used directly and also methanol, distilled water were used as a solvent in sol – gel process.

➢ *Characterization*

Powder X-ray diffraction pattern was obtained from a Rigakuminiflex diffract meter for 2ɵ values from 10^0 to 90^0 using Cukα target at wavelength of $\lambda = 1.5406A^0$. The FTIR analysis was carried out in a Perkin Elmer Spectrum 1000 using the KBr pellet method. The UV-Vis spectra were recorded with a Hitachi, UV3501 spectrometer. Scanning electron microscopy (SEM), (JEOl – JSM – 6360LV) was used to record the morphology of the prepared materials and the elemental analysis was carried out by energy dispersive analysis (EDX) and Treated rice husk ash TGA and DTA analysis were performed in thermo gravimetric equipment (Pyris7, Perkin – Elmer).

A. Experimental Procedures

➢ *Preparation of Rice Husk Ash*

Silica was extracted from Ragi husk ash (RaHA), the procedure was given in our earlier paper [Geetha et al., (2016)].

➢ *Preparation of silica gel nano particles*

Preparation of silica gel from rice husk ash, the procedure was given in our earlier paper [Geetha et al., (2016)].

$$SiO_2\,(Ash) + 2NaOH \longrightarrow Na_2SiO_3 + H_2O \quad \text{----------} (1)$$

ISSN No:-2456-2165 https://doi.org/10.38124/ijisrt/IJISRT24SEP075

$$Na_2SiO_3 + H_2SO_4 \longrightarrow SiO_2 + Na_2SO_4 + H_2O \quad \text{---------- (2)}$$

During the addition of sulphuric acid, Si-OH formed and condensed to form siloxane bond as shown below

$$Si-OH + HO-Si \longrightarrow Si-O-Si + H_2O \quad \text{---------- (3)}$$

➢ *Synthesis of RHS doped Titania:*

The synthesis of titania – silica nano composites was prepared by sol – gel method. The molar ratio of silica to titania sols was 0.5:0.02. The main solution added step by step another solution 5 hrs for stirring, finally the gel was seen. This gel for one day was aged for one day and followed by temperature at 150^0C for 5 hrs. Lastly the mixture was filtered and dried at oven. The resultant product was noted at RHS-TiO_2.

➢ *Synthesis of RHS/TiO_2/Ni Nano Composites:*

The preparation of RHS/TiO_2 nano composites doped nickel by using sol – gel technique. The Stock solution was added to titania (0.5:0.02) solution while stirring for 30 minutes and immediately added to nickel solution (varying concentrations are 0.5,1.0,1.5%wt) within a fraction of time the product was seen. The wet gel was dried kept at hot air oven. The finally product labelled RHS/TiO_2/Ni.

B. Phase Investigation and Structural Analysis:

In Fig 1(a), the sample is whole is in amorphous as pointed out by the featureless diffract grams and the appearance of a scatter maximum at $2\theta = 23^0$ characteristic for amorphous silica [14]. This pattern exhibits a very broad line and no defined peaks due to crystallinity were encountered. On the figure 1(a) are also described the theoretical postures of the main reflexion of the phase cristobalite (SiO_2) and graphite (C) and no peaks were discovered in the XRD. These entire spectra were clearly noted that the ash was produced and this structure is amorphous. [15]

➢ *RHS Doped TiO_2*

In Fig 1(b) RHS doped with TiO_2 (1:1) agrees the main peak $2\theta = 25.28^0$ corresponding to (101) plane and it is the strong peak of anatase (JCPDS 21-1272). The other main two diffraction peaks at 25^0 and 48^0 indicating TiO_2 in the anatase structure. Amorphous disclosed a broad pattern with low intensity. Silica can exhibit the formation anatase by impeding direct contact between TiO_2 particles forming the Ti – O – Si binding [16]. The diffract gram indicating that only anatase phase has been formed. The use of TiO_2 in the half of the silica matrix will reduce the anatase phase and forming amorphous TiO_2 – SiO_2 [17].

➢ *Nickel Doped RHS/TiO_2*

In Fig 1(c-e) Nickel was doped (0.5, 1.0 and 1.5 % wt) RHS/TiO_2 to form a hybrid nano composite. It clearly shows that, some of the peaks are very low and less broad. The levels of Ni doping increasing from 0.5, 1.0 and 1.5 %wt some of the variations were observed. It clearly suggest that nickel up to a 1.5%wt, restored some places of titanium ions in TiO_2 lattice (or) occupy interstitial positions of TiO_2crystal structure (or) remaining on the surface of TiO_2 as a single lamella uni molecular oxide amorphous mono layer.

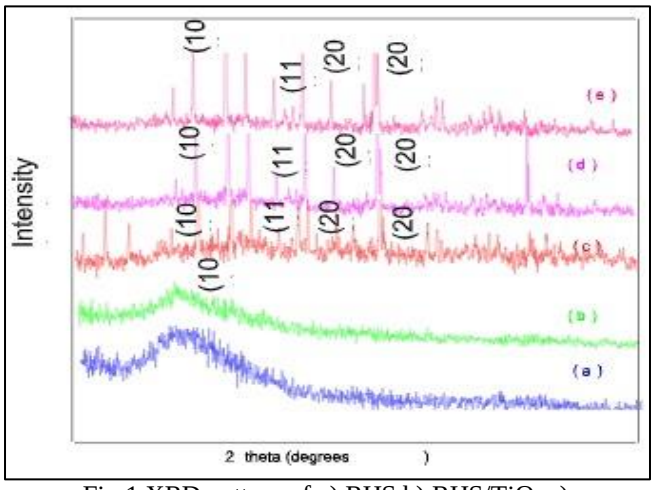

Fig 1 XRD pattern of a) RHS b) RHS/TiO_2 c) RHS/TiO2/0.5Ni d) RHS/TiO2/1.0Nie) RHS/TiO2/1.5Ni

It is evidence that the size of the sample decreases with adding dopant concentration of nickel. Also it is evidence that the particle agglomerates due to van der Waals forces and they are responsible for ultrafine nickel nanoparticles. The crystal structures of the samples are FCC. From the XRD pattern, the most intense peak was observed at $2\theta = 43.89^0$(JCPDS 47 - 1049) and the corresponding plane (200) and confirmed nickel doped RHS/TiO_2. The mean particle size was calculated by using Debye Scherer Formula, the undoped anatase TiO_2 powder possesses particle size was 42.24nm. When dopant concentration was increased to 1.5%, the particle size value further decreases [18]. These results suggest that Ni below 1.5% doping concentration effectively inhibits TiO_2 grain growth probably by staying at grain boundaries thereby decreasing the particle size. The decrease in grain growth can also be attributed to the formation of Ni – O – Ti bonds in the dopant powders, which inhibits in the growth of the crystals. However, as the Ni concentration increased further to 0.5, 1.0 and 1.5%, the particle size decreased respectively, to 38.68, 26.11 and 18.60nm.

➢ *Morphology Index:*

It is already well known that the RHS doped titania nano powder used for lot of industries, various properties of physicochemical by its hardness, surface properties and also concluded that particle size. It is clearly seen that nanocomposite of TiO_2 rely the size of the particle and morphology. Morphology index is calculated from Full width half maximum of XRD to explore this relationships, Morphology index is acquired using equation,

$$MI = \frac{FWHMh}{FWHMh + FWHMp} \quad \text{---------- (3)}$$

Where,

$FWHM_h$= is the highest full width half maxima value acquired from peak

ISSN No:-2456-2165 https://doi.org/10.38124/ijisrt/IJISRT24SEP075

$FWHM_p$ = is the full width half maxima value particular peak

Morphology index values are presented in table1. It is noted that MI is increasing with increased particle size. The results are shown in Fig4. Linear fit exhibits the deviations and the relationships between them. The observations values confirmed that some of the parameters of the prepared samples and the values are tabulated (1).

➢ *Dislocation Density*

The presence of dislocation strongly influences physical, thermal, mechanical and chemical properties. Mathematically, it is one of the types of topological defect. Chen and Hendrickson resolved dislocation density and hardness of several silver crystals. It is clearly seen that the dislocation density is inversely proportion to the grain size, strain and also various parameters noted it.

The dislocation density of the sample has been measured by using eqn (4) and eqn (5)

$$\Delta = \frac{15\beta\cos\theta}{4\alpha D} \quad \text{---------- (4)}$$

$$\Delta = 1 / D^2 \quad \text{----------(5)}$$

Where, δ – Dislocation density, β – diffraction broadening – measured at half of its maximum intensity (radian), θ – diffraction angle (degree), α – lattice constant (nm) and D – particle size (nm). Dislocation density increases while particle size decreases.

➢ *Strain:*

Elastic strains are also calculated from spectra of XRD. It evidence that tiny particles have high strain and also large particles have low strain. These values are verified the literature value. The values are tabulated (1).

Table 1. Particle Size and Dislocation Density of the Nano Composites

Sample Name	Particle size (Debye) nm	Particle size (W-H plot) nm	Strain Unit less	Dislocation Density (m^2)
RHS	50.42	69.32	0.002	0.638 X 10^{-15}
RHS/TiO_2	22.04	54.32	0.002	0.541 X 10^{-15}
RHS/TiO_2/0.5% Ni	38.68	48.14	0.004	0.307 X 10^{-15}
RHS/TiO_2/1.0% Ni	26.11	43.18	0.005	0.513 X 10^{-15}
RHS/TiO_2/1.5% Ni	18.60	40.21	0.011	0.801 X 10^{-15}

C. Spectral Studies:

Fig 2(a) shows an FTIR spectrum at RHS. A broad band in the range of 3362 cm^{-1} is due to the stretching vibration of the O – H band and is due to silanol groups. The weak band 1642 cm^{-1} is assigned to H – O – H bending vibrations mode where also represented due to the adsorption of water in air. Also, there is a tiny dip in the spectra at 2354 cm^{-1} due to the presence of atmospheric CO_2. These peaks are trapped in the matrix of silica surface. The predominant peak at 1383 cm^{-1} is due to silicone bonds (Si – O – Si). The adsorption bands between 474 and 993 cm^{-1} are because of silica structures and other peaks observed in the range of 1247 and 2764 cm^{-1} are because of impurities such as carbonate and sodium groups. The peaks between 1055 and 711 cm^{-1} indicates the vibration modes of Si – O – Si network. A most intense band at 1110 cm^{-1} and a peak 765 $cm^{-1}$are due to asymmetric and symmetric stretching mode at Si – O – Si. The bending vibration of Si – O is shown by strong band at 475 cm^{-1}.

➢ *RHS Doped TiO_2*

In Fig 2(b) the presence of some weak transmittance bands between 3362 &3467 and at a 1634 are seen, which are gradually decreased with TiO_2 doping concentrations. An intense band at 606 and 852 cm^{-1} is seen which is attributed to different vibrational modes of TiO_2. The intense band below 1343 cm^{-1} is due to Ti – O – Ti vibrations. The shift in lower wave numbers and sharpening of the Ti – O – Ti band width increase of TiO_2 concentration could be attributed to the decrease of particle size. The band 835 cm^{-1} are mainly ascribed to Ti- O and Ti – O – O bonds. The proposed mechanism for Ti – O – Si bond formation can be explained as the following reactions.

$$Ti(OC_4H_9)_2 + C_2H_5OH \longrightarrow Ti - OH \text{ (Hydrolysis reaction) -------- (6)}$$

$$SiO_2 + C_2H_5OH \longrightarrow Si - OH \text{ ---------- (7)}$$

$$Ti - OH + Ti - OH \longrightarrow Ti - O - Ti \text{ (Condensation without Si) ----- (8)}$$

$$Si - OH + Si - OH \longrightarrow Si - O - Si \text{ (Condensation without Ti) ------(9)}$$

$$Ti - OH + Si - OH \longrightarrow Ti - O - Si \text{ (Condensation with the combination of Ti and Si) ---------- (10)}$$

ISSN No:-2456-2165 https://doi.org/10.38124/ijisrt/IJISRT24SEP075

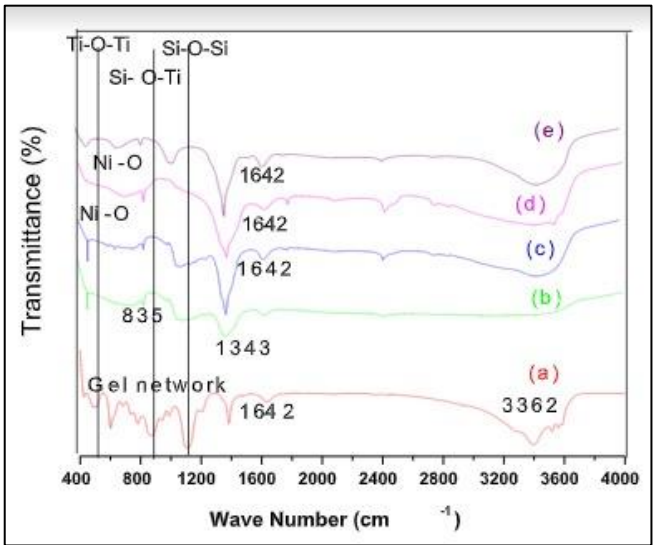

Fig 2 FTIR Spectra of a) RHS b) RHS/TiO_2 c) RHS/TiO2/0.5Ni d) RHS/TiO2/1.0Nie) RHS/TiO2/1.5Ni

➢ *Nickel Doped RHS/TiO_2*

In fig 2 (c-e) Nickel doped with RHS/TiO_2 (0.5, 1.0 & 1.5%wt) respectively. The band 466 cm^{-1} confirmed that the NiO nanoprticles. In spite of drying this sample contained trace of water molecules. The broad adsorption band 685 and 710 cm^{-1} is assigned to Ni – O stretching vibration mode, the broadness of the adsorption band indicates that the NiO powder. The adsorption of CO_2 from the atmosphere at the NiO surface was indicated from sharp peak positioned at about 1631 cm^{-1} in FTIR spectra. The 475 cm^{-1} indicated that the vibration band of Ni O [21].

D. Thermal Studies:

In fig (3), the total decomposition behaviour of RHA was attributed to decomposition of hemicelluloses, cellulose and lignin. In this figure, it was noted that there was a decrease in the temperature of the sample around 200^{0}C.

The sharp decrease in weight over a temperature range of 150^{0}C can be attributed to the thermal combustion of organic groups present in the ash and rapid decomposition of the sample.

$$\text{Rice Husk} \longrightarrow \text{Intermediate + Volatiles} \quad \text{---------- (11)}$$

In DTA curve, there are two exothermic peaks at 250^{0}C and 450^{0}C which are correlated to the removal of organic groups by oxidation and sudden decomposition of the sample respectively [22]. In Fig (4) TG – DTA for RHS/TiO_2, curve of the mass loss occurring in the range from 180^{0}C to 310^{0}C may be attributed to the decomposition of organic and inorganic materials. The final step clearly noted, elimination of water molecule 200^{0}C and decomposed of $Ni(OH)_2$ to NiO nanoparticles as shown in fig (5). When the temperature is above 400^{0}C weight loss fairly nano composites $Ni(OH)_2$. $5H_2O$ represented as

$$Ni(OH)_2.5H_2O \quad Ni(OH)_2 \quad NiO \quad \text{-------- (12)}$$

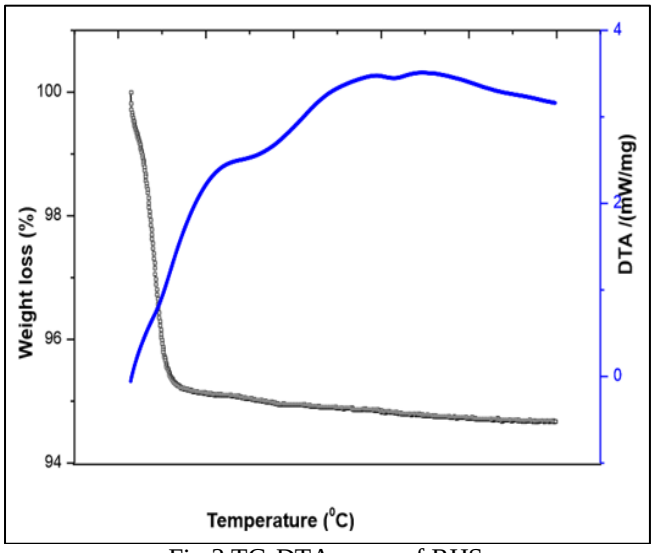

Fig 3 TG-DTA curve of RHS

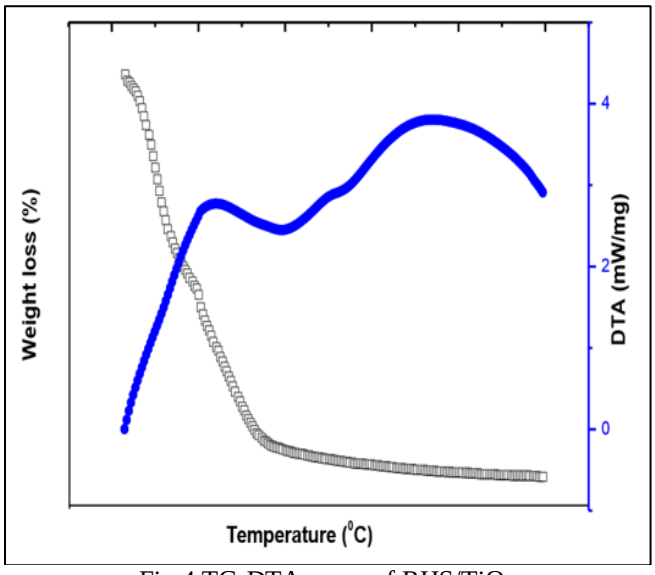

Fig 4 TG-DTA curve of RHS/TiO_2

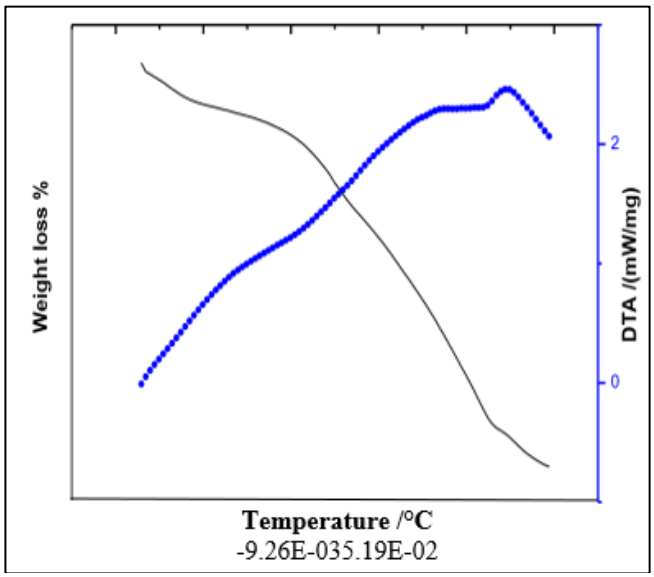

Fig 5 TG-DTA curve of RHS/TiO_2

ISSN No:-2456-2165 https://doi.org/10.38124/ijisrt/IJISRT24SEP075

E. Morphology Studies:

Fig 6(A and B) exhibited the SEM/EDX spectrum of RHS. In view of this image, RHA particles are shaped in polygonal. The EDS spectrum noticed that silica in higher percentage [23]. Fig 6(C, D) characterized RHS/TiO_2. The forming agglomeration because of silica and titania phase, it prevents the formed boundaries of silica in amorphous phase. It evidence that Ti, O and Si are present in the sample [24]. The surface morphological features of synthesized Nickel doped RHS/TiO_2 nano composites were studied by SEM in Fig 6(E) & (F).

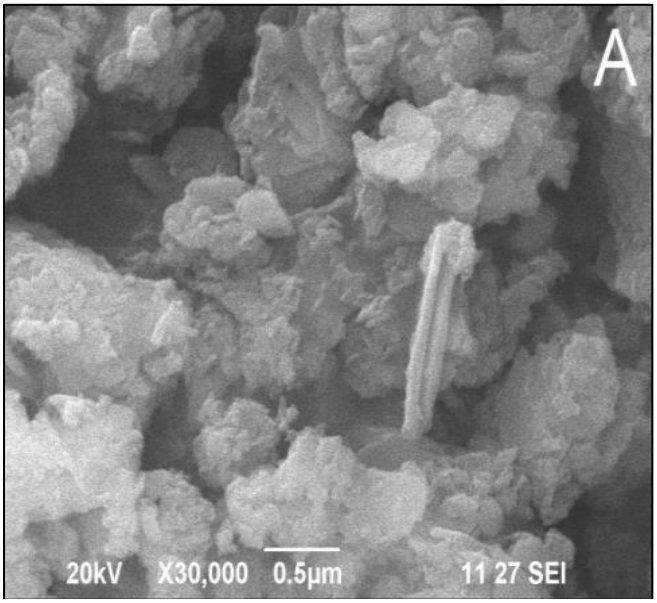

Fig 6 (A) SEM Image of RHS

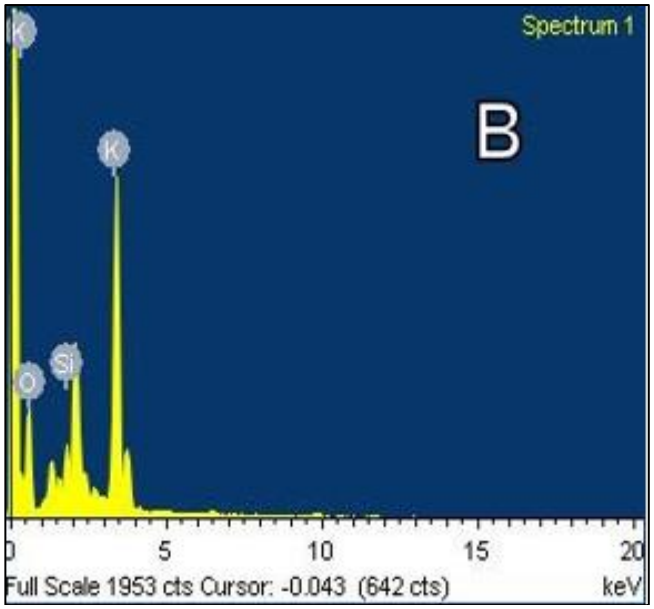

Fig 6 (B) EDS Spectrum of RHS

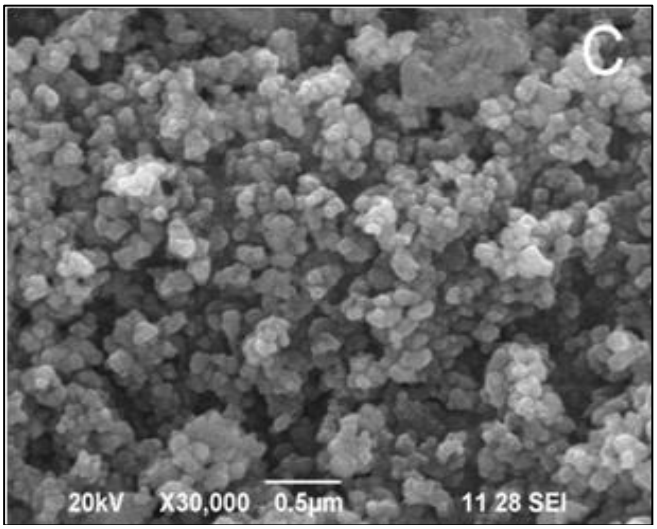

Fig 6 (C) SEM Image of RHS/TiO_2

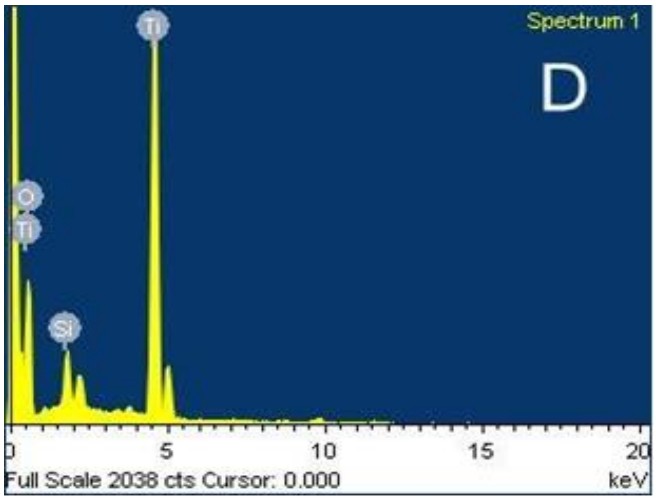

6 (D) EDS Spectrum RHS/TiO 2

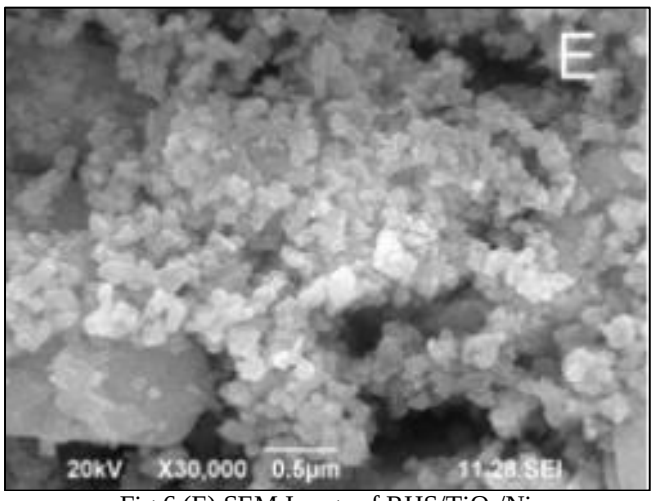

Fig 6 (E) SEM Image of RHS/TiO_2/Ni

ISSN No:-2456-2165 https://doi.org/10.38124/ijisrt/IJISRT24SEP075

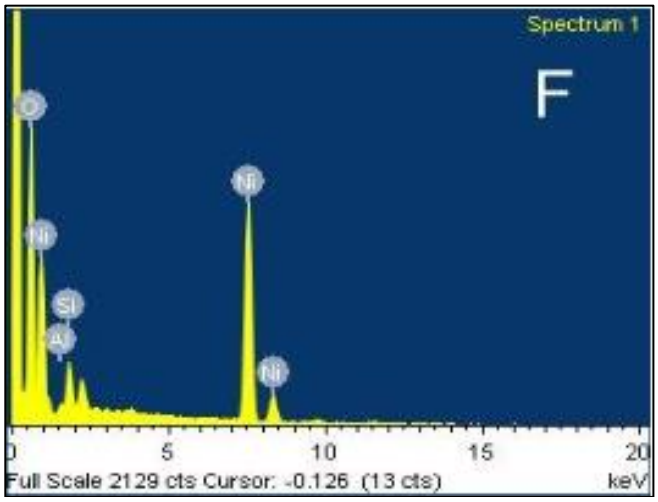

Fig 6 (F) EDS Spectrum of RHS/TiO_2/Ni

The result indicates that mono – dispersive and highly crystalline RHS/TiO_2/Ni nano composites are obtained. The appearance lot of particles are seen by spherical shape. It mentions that the particles are highly agglomerated and they are essentially cluster of nano composites. The images exhibit the size of poly crystalline composites. Nano composites have the tendency to agglomerate due to their high surface tension of the ultrafine nano composites. Fig 6(F) shows the EDX analysis of the product Ni, Si, O and Ti signals come from RHS/TiO_2/Ni nano composites.

F. Optical Studies:

Before studying the photo catalytic activity SiO_2 doped TiO_2, UV image was concluded that the experiment. The broad band when increasing SiO_2 290 nm was seen that shift of blue. The highest wavelength UV absorption was obtained for the sample RHS: TiO_2 (50:50) having peak at approximately 330nm which is less than that Rice husk ash. From Fig 18(a) UV – Vis spectra of RHS/TiO_2/Ni nano composites is quite different from that of the starting material, confirming that the strong band appeared at 320 nm due to NiO nano composites not Ni^{2+}. The solvent plays a vital role to the reduction and nature of the product. The main peak around 300 nm exhibited to the originated it. The balanced peaks are attributed to near band to band related imperfections.

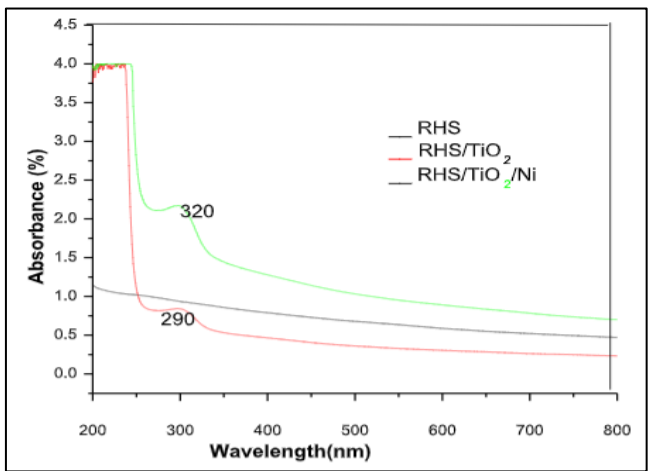

Fig 7 UV-Vis Spectrum for RHS/TiO_2/Ni

III. CONCLUSION

According to the results and discussions presented above, a bio based product of new one type of Ni doped RHS/TiO_2. These potential catalysts were successfully prepared through the sol –gel route. The interaction between metal and silica behaved to be via strong chemical metal oxygen bonding. The particle size was noted inversely proportional to the doping concentrations. XRD has also verified also some of the characters were calculated. The porous structure of titania decreased proportionally with increasing concentration of the dopant. Nickel was found to be effectively doped on the surface of RHS/TiO_2 samples. EDS analysis of Ni doped RHS/TiO_2 confirmed that in the spectrum. The Ni doped RHS/TiO_2 acquired via doping of selected dopants are characterized by a shift change in thermal stability. This preparation method was also used for future synthesis of transition of metal oxides.

REFERENCES

[1]. Umeda J, Kondoh K and Michiura Y. Process parameters optimization in preparing highpurity amorphous silica originated from rice husks. *Materials Transactions*. (2007) 48(12):3095- 3100.

[2]. Shen J, Liu X, Zhu S, Zhang H and Tan J. Effects of calcination parameters on the silica phase hydrolysis: effects of original and leached rice husk ash. *Materials Letters*. (2011) 65(8):11791183

[3]. Wang W, Gu B, Liang L, Hamilton WA, Wesolowski DJ. Synthesis of rutile nanocrysttals with controlled size and shape by low temperature hydrolysis: effects of solvents composition.J.Phys.Chem.B. (2004)108, 14789-92

[4]. Bak T, Nowonty J, Rekas M, and Sorrell C.C., Review article: Photo electrochemical hydrogen generation from water using solar energy. Materials related aspects, International journal of hydrogen energy, (2002), 991-1022.

[5]. Gole J.L., Prokes, S.M., Glembocki O. J, Wang J, Qiu X and Burda C, study of concentration dependent cobalt ion doping of tio2 and tio22-x Nx at the nanoscale, Nanoscale, (2010), 11341140.

[6]. 6.Lin, Y.J, Chang Y.H., Yang W.D., and Tasi B.S., synthesis and characterization of ilmenite NiTiO3 and CoTiO3 prepared by a modified by pechini method, journal of non – crystalline solids, (2006), 789-794.

[7]. Devi L.G., Kottam .N., Kumar S.G., and Rajashekhar K.E., preparation and enhanced photocatalytic activity of Ni2+ doped titania under solar light, Central European journal of chemistry, (2010), 142-148.

[8]. Bengum N.S., Ahmed H.M.F., Gunasekhar.g., effects of Ni doping on photocatalytic activity of TiO2 thhinfilms prepared by liquid phase deposition technique, Bulletin of materials science, (2008), 747-751.

[9]. Nozik A.J., photochemical diodes, U S patent No.4,094,751, (1976), 150-153.

ISSN No:-2456-2165 https://doi.org/10.38124/ijisrt/IJISRT24SEP075

[10]. Shu X, He J, Chen D, Visible light induced photocatalyst based on the nickel titanate nanoparticles, Industrial and engineering chemistry research, (2008), 4750-4753.
[11]. Krivtsov, Ilkaeva I.V., Samokhina V.D., Khainasov S.A., Uchaev D.A., Effects of transition metal doping on the growth and properties of rutileTiO2 Nanoparticles, J.Sol-gel Sci.Technol., (2013), 665-669.
[12]. 12.Adam F, Andas, J.Amino benzoic acid modified silica – An improved catalyst for the monosubstituted product ofbenzylation of toluene with benzyl chloride, J. colloid interface, (2007), 135-143.
[13]. Kalapathy U, A. Proctor, J. Shultz, A simple method for production of pure silica from rice hull ash, M. Chareonpanich, Bioresour. Technol. 73 (2000) 257–262.
[14]. Della V.P., I. Kühn, D. Hotza, Rice husk ash as an alternate source for active silica production, Mater. Lett. 57 (2002) 818–821.
[15]. Watari J, A. Nakata, T. Torikai, M. Yada, Fabrication of porous SiO2/C composite from rice husks, Journal of the European Ceramic Society 26 (2006) 797–801.
[16]. Conradt R, P. Pimkhaokham, U. Leela-Adisom, Nano-structured silica from rice husk, Journal of Non-Crystalline Solids 145 (1992) 75–79.
[17]. Park B.D., S. Wi, K. Lee, A. Singh, T.-H. Yoon, Y. Kim, Characterization of anatomical features and silica distribution in rice husk using microscopic and micro-analytical techniques, Biomass and Bioenergy 25 (2003) 319–327.
[18]. Ayhan, Demirbas, A discussion of the paper "Study on the pozzolanic properties of rice husk ash by hydrochloric acid pre-treatment" by Q. Feng, H. Yamamichi, M. Shoya, S. Sugita, Cement and Concrete Research 35 (2005), 1017.
[19]. Yuvakkumar R, V. Elango , V. Rajendran& N. Kannan, High-purity nano silica powder from rice husk using a simple chemical method, Journal of Experimental Nanoscience, (2014).
[20]. Nabeel A. Bakr*, Sabah A. Salman, Ahmed M. Shano, Effect of Co Doping on Structural and Optical Properties of NiO Thin Films Prepared By Chemical Spray Pyrolysis Method**,** *International Letters of Chemistry, Physics and Astronomy, 11, 2014, 15-30.*
[21]. Rajinder Kumar, Ragini Raj Singh and P. B. Barman, COBALT DOPED NICKEL ZINC FERRITE NANOPARTICLES – XRD analyses an insight **,** International Journal of Scientific & Engineering Research, 5(5),(2014).
[22]. Theivasanthi T, and M. Alagar , X –ray diffraction studies of coper nano powder,.
[23]. ThirugnanasambandanTheivasanthi* and MarimuthuAlagar, Titanium dioxide (TiO_2) Nano particles – XRD Analyses – An sight.
[24]. SelvarajVentakeswaran, Ratinamyuvakumar and Venkatachalamrajendran, Nano silicon from nano silica using natural resource (Rha) for solar cell fabriciation, Phosphorus, sulphur and silicon and the related elements, (2013), 1178-1193.